Control of impurity diffusion in silicon by IR laser excitation

2007 J. Phys.: Condens. Matter 19 365207

(http://iopscience.iop.org/0953-8984/19/36/365207)

IOP PUBLISHING JOURNAL OF PHYSICS: CONDENSED MATTER

J. Phys.: Condens. Matter **19** (2007) 365207 (7pp) doi:10.1088/0953-8984/19/36/365207

Control of impurity diffusion in silicon by IR laser excitation

K Shirai[1], **H Yamaguchi**[1] **and H Katayama-Yoshida**[1,2]

[1] Nanoscience and Nanotechnology Center, ISIR, Osaka University, Mihogaoka 8-1, Ibaraki, Osaka 567-0047, Japan
[2] ISIR, Osaka University, Mihogaoka 8-1, Ibaraki, Osaka, 567-0047, Japan

E-mail: koun@sanken.osaka-u.ac.jp

Received 13 December 2006, in final form 29 January 2007
Published 24 August 2007
Online at stacks.iop.org/JPhysCM/19/365207

Abstract

Control of the diffusion of a specific impurity species is desirable in Si device processes. IR laser excitation matching the impurity vibration mode is a promising method for this purpose. To illustrate the effectiveness of this method, first-principles molecular dynamics simulation has been applied. Technical issues of the simulation are described in detail. It is seen that resonant effects can be reproduced in adiabatic molecular dynamics simulations by applying an external force on the impurity only. The present study forms the basis for further developments of this approach.

(Some figures in this article are in colour only in the electronic version)

1. Introduction

Control of impurity diffusion is an important element in present-day device technologies [1, 2]. The usual thermal processes have a major disadvantage in that not only the intended species but also all other impurities involved are equally affected. This imposes many restrictions on the device process. To remove such restrictions, it would be desirable to diffuse the specific species only. If such a technique of selective diffusion could be established, the impact on the device industry would be great.

One such attempt is the use of infrared (IR) excitation [3]. The idea is that every impurity has its own local vibration in the host crystal. The frequency of vibration is dependent on the impurity species. Irradiation by an IR laser with the resonant frequency could cause excitation of the local impurity modes resulting in the selective enhancement of diffusion of that impurity. Unfortunately, such IR excitation experiments are difficult because of the lack of available IR lasers with suitable frequencies. We temporarily ignore this technical difficulty in the hope that IR sources with a variety of frequencies will be available in the near future. At present it is rather important to show by simulation the effectiveness of IR excitation in order to motivate experimentalists to research this subject.

First-principles molecular dynamics (FP-MD) simulation for diffusion is still difficult in terms of timescale. Sufficient simulation time and a sufficient ensemble average are required, which severely restricts the feasibility of applying this technique to real problems. That is why very few FP-MD simulations have been performed since Buda *et al* first applied it to the problem of H diffusion in Si [4]. Hydrogen is an exception in that it diffuses very rapidly. Recently, the authors have applied this technique to the diffusion of Cu in Si [5]. This example is also an exception because Cu has exceptionally fast diffusivity. The timescale problem does not invalidate the utility of classical model simulations.

Besides the problem of timescale, diffusion phenomena essentially consist of anharmonic motion of atoms. An accurate description of the adiabatic potentials is required, which is beyond classical model calculations. In addition, strong laser excitation suggests strong anharmonic phenomena. In this situation, the power of predictability achievable with FP calculations is indispensable. At this point, we compromise with the timescale problem, focusing primarily on an aspect of the elemental process of atomic excitation. The size of the resonance that occurs in atomic displacement is the present concern.

In this paper we examine FP-MD simulation for IR excitation from the above point of view. First, we present a simulation model of IR excitation, because it is rare to treat IR excitation by FP-MD simulation. Technical details of the calculations then follow. In particular, thermocontrol is an important ingredient. A few preliminary results are illustrated. Worked examples are given for O, B and P impurities in silicon.

2. MD simulation

2.1. Scale of the simulation

Let us begin by setting the scale of the simulation which is required for the present problem. The magnitude of the resonant effect is primarily determined by the line width γ of vibration (or the lifetime of the phonon τ_p). A smaller line width means a more effective resonance. The typical value of γ for local vibration modes is of the order of 1 cm^{-1} [6–9], although of course the value can deviate from this order significantly depending on the material. This requires the resolution of frequency in MD simulation being at least 0.1 THz, which amounts to a simulation time of 10 ps. This is almost the upper limit of FP-MD simulation given the present status of calculation techniques.

In addition, the calculation of an accurate line width requires the accurate DOS of phonons, because the phonon lifetime depends on the phonon DOS (two-phonon DOS in the lowest order) [10]. The energy resolution of the phonon DOS obtained by the super-cell method is limited by the size of the super cell. Large super cells are desirable for calculating the line width. Furthermore, many runs of MD simulation are required in order to make the result statistically meaningful. It is impossible to satisfy all these requirements with the present status of FP-MD simulations. As stated earlier, we seek restricted aspects of FP-MD simulations.

We set the simulation time as typically 9.7 ps, which gives a frequency resolution of 3.4 cm^{-1}. This is marginal for resolving line widths of local vibration modes. The time step Δt is set to be 2.42 fs. The size of the super cell is 16 atoms per cell. This is indeed very small compared to the typical size of static calculations in the literature. But by reducing the size of the super cell we get the benefit that many MD runs are possible.

FP-MD simulations are performed using the pseudopotential method with the plane-wave basis. The code used is 'Osaka2k'. The local density approximation is employed and the Perdew and Zunger parameterization form is used for the exchange–correlation functional [11]. Norm-conserved pseudopotentials of the Troullier and Martins type are used [12], with the help

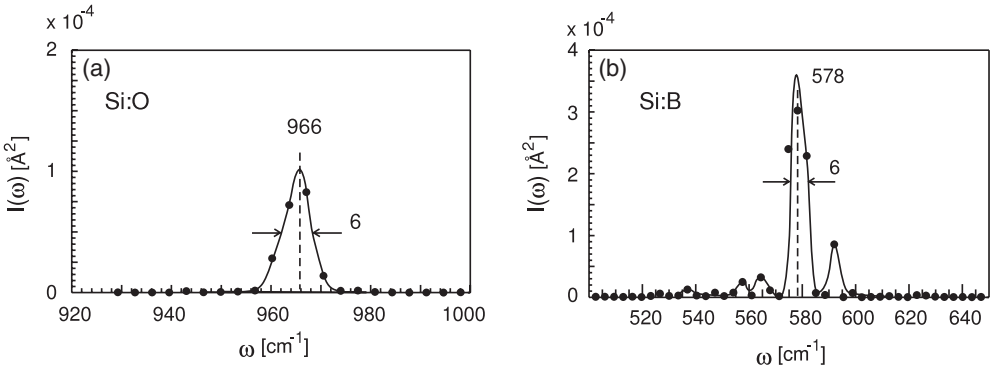

Figure 1. Line shape of impurity bands in Si obtained by MD simulation: (a) oxygen, (b) boron. Simulations were performed on a 16-atom super cell containing an impurity atom. The simulation time was 9.7 ps. The average temperature was about 300 K.

of the Kleinman and Bylander fully separable form [13]. Further details can be found in the user manual [14].

Figure 1 shows the line shape of the local vibration mode obtained with the MD simulations. The figure shows the spectra of O and B impurities in Si in the form of power spectra of displacement $I(\omega)$. The calculated frequency of the local vibration mode is, more or less, deviated from the experimental value. For the O mode, the frequency is experimentally obtained to be 1136 cm^{-1} for ^{16}O and 1109 cm^{-1} for ^{18}O [9]. For B, the local vibration mode is found at 517 cm^{-1} just below the host TO mode (520 cm^{-1}), so that the band has been assigned as an in-band resonance mode [15]. In our simulation, the frequency is higher than the host TO mode. For the line width γ, a value of 6 cm^{-1} is obtained in the calculation for both O and B modes. The experimental values are 0.6 cm^{-1} for ^{16}O and 1.2 cm^{-1} for ^{18}O [9].

There are some discrepancies between MD simulation and experiment. These discrepancies might be ascribed to the size of the super cell being too small. But such a large discrepancy is sometimes found in other MD simulations with large super cells [16]. We shall defer discussion of the discrepancies until later. Rather, we shall now concentrate on systematic variation in the frequency and the line width.

2.2. Introduction of a bias force

FP simulation of laser irradiation of solids is a currently active field. Time-dependent density-functional theory [17] is suited to this problem, and accordingly real calculation methods have been developed [18]. To solve the time-dependent KS equation, however, is very computationally demanding; we could not even reach several tens of femtoseconds in MD simulations.

In this study, we use the usual method of adiabatic MD simulation; wavefunctions are treated as being in steady states. Treatment of the applied electric field is a cumbersome problem in periodic systems [19–22], so to avoid this we made a phenomenological treatment to introduce a bias force f_{ext} on the impurity atom under consideration only. The local electric field E_{loc} may be obtained from f_{ext} by a correction of the effective charge of impurity e^*. But the calculation of the local-field correction itself is very complicated. We circumvent this problem by always treating the external force as the controlling quantity, leaving the electric field to be determined by further calculation.

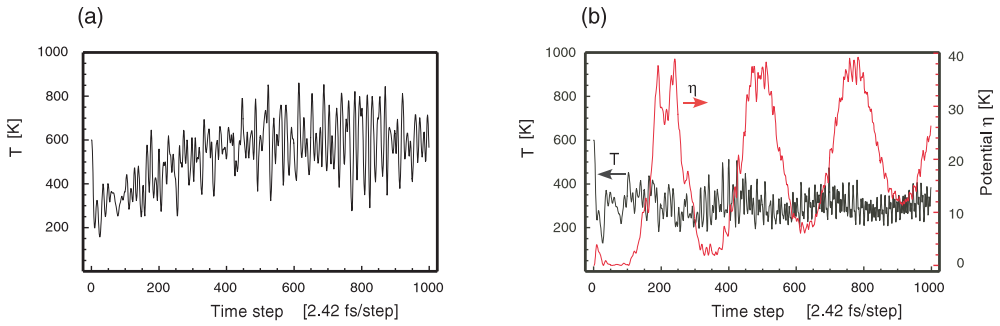

Figure 2. (a) Time evolution of the system temperature $T(t)$ for a $Si_{15}B$ super cell, when an external force is applied to the B atom, $f_0 = 8.9 \times 10^{-3}$ Ryd/bohr and $\omega_{ext} = 580$ cm^{-1}. No thermocontrol is done, so that the initial kinetic energy determines the subsequent motion of the system; $T(0) = 600$ K. (b) Time evolution of the system temperature $T(t)$ when the Nosé thermostat is used; $Q = 10$ au and $T_{bath} = 300$ K. The red line shows the Nosé potential, $3kT_{bath}\eta$ in K.

This bias technique was applied to a problem of impurity diffusion by the present authors [23] in order to accelerate the process. In that case, the applied force was simply a constant (DC) force. In the present case, the applied force is a monochromatic (AC) force with a frequency ω_{ext},

$$f_{ext}(t) = f_0 \exp(i\omega_{ext}t)\,. \tag{1}$$

The applied frequency ω_{ext} is adjusted to the impurity mode under consideration. The strength of the applied force f_0 is a controlling parameter, and is kept constant during a MD run, typically of the order of 10^{-2} Ryd/bohr. This amounts to extremely strong laser excitation: $E = 5.1 \times 10^7$ V m^{-1} and $I = 3.51 \times 10^{12}$ W cm^{-2}, provided $e^* = 1$. For the layout of the experiment, the strength of the force is important and should be carefully considered.

2.3. Thermocontrol

Since we artificially apply an external force on an impurity, our system is not an energy-conserving system. If the size of the super cell were large, the influence of the external force would be negligible. But since the cell size in the present case is so small this may really be a concern for the numerical stability of the MD simulation. Hence, the evolution of the energy of the system should be examined.

Figure 2(a) shows the time evolution of the instantaneous temperature of the super cell containing a B impurity. The instantaneous temperature $T(t)$ is defined by the average of the atom kinetic energy at a time t. As seen, T increases during the course of time. If we left it alone, our MD simulation would eventually collapse. Clearly, thermocontrol is desirable. The easiest way to achieve thermocontrol is by velocity scaling. But this method is not suited for the present purpose, for the same reason as for the acceleration of diffusion problem [23]—the velocity scaling negates all efforts at excitation.

Instead, a Nosé thermostat [24] is used. An example with T_{bath} set at 600 K is shown in figure 2(b). As shown in the figure, the injected energy is successfully absorbed in the Nosé heat bath while still allowing the impurity atom to be accelerated at a suitable level. Instead of this desirable feature, it is noted that the Nosé thermostat introduces a further complication: phonon decay processes occur through this artificial heat bath. The typical response frequency

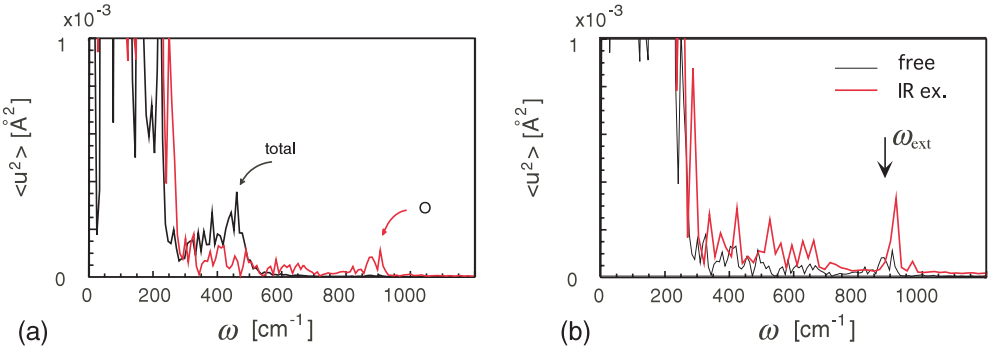

Figure 3. The resonance effect on the oxygen impurity mode. The left figure (a) shows the natural spectrum of the $Si_{16}O$ system without IR irradiation; the black (thin) curve shows the average $\langle |u_i(\omega)|^2 \rangle$ of the power spectra over all the atoms, while the red (thick) curve shows the oxygen (i = O) component. The right figure (b) shows the change in the $|u_i(\omega)|^2$ of the O mode due to IR irradiation; the black (thin) curve shows a power spectrum without irradiation, while the red (thick) curve shows that with irradiation. In both cases the average temperature is set to be about 1000 K.

of a Nosé thermostat is about 1.5 THz, which lies in the low-energy tail of the host phonon spectrum.

3. Preliminary results

3.1. Local modes

Simulation of IR excitation was examined for an O impurity in a 16-atom Si super cell. The O atom was placed at the bond centre, with atom relaxation, which allows the bond to bend. Let us check the whole spectrum of vibrations when no IR excitation is applied. Figure 3(a) shows the power spectrum $|u_i(\omega)|^2$ of the displacement of the ith atom. The power spectrum is obtained by Fourier transformation of the atom displacement $u_i(t)$ as a function of t, which is obtained directly by MD simulation. The power spectrum is related to the usual phonon DOS $g(\omega)$, as

$$\tfrac{1}{2}\sum_i M_i\omega^2|u_i(\omega)|^2 = \left[n(\omega)+\tfrac{1}{2}\right]\omega g(\omega), \tag{2}$$

where $n(\omega)$ is the Bose factor. Accordingly, the power spectrum reflects not only the pure phonon DOS $g(\omega)$ but also the magnitude of the displacement through the Bose factor. The usual phonon DOS $g(\omega)$ of Si has two peaks with almost the same intensity; one is the optic branch around 500 cm^{-1} and the other is the acoustic branch at less than 200 cm^{-1}. As can be seen, in the form of $|u_i(\omega)|^2$ the amplitude of the low-frequency side is significantly magnified because of the Bose factor. The O component clearly has a local mode at about 930 cm^{-1}, much above the host spectrum.

Now we apply an external force on the O atom in this super cell, with the frequency ω_{ext} = 930 cm^{-1}. The change in the power spectrum is shown in figure 3(b). As seen, the displacement of the O atom is significantly amplified. The resonance effect is evident.

Because the stretching mode of O is a typical local mode, the resonant effect is appreciable. This resonance effect is also appreciable for the B mode. In the case of P, the impurity mode is buried in the host phonon band, so that the resonance effect is not appreciable. Details of the effect in individual cases will be described in a forthcoming paper.

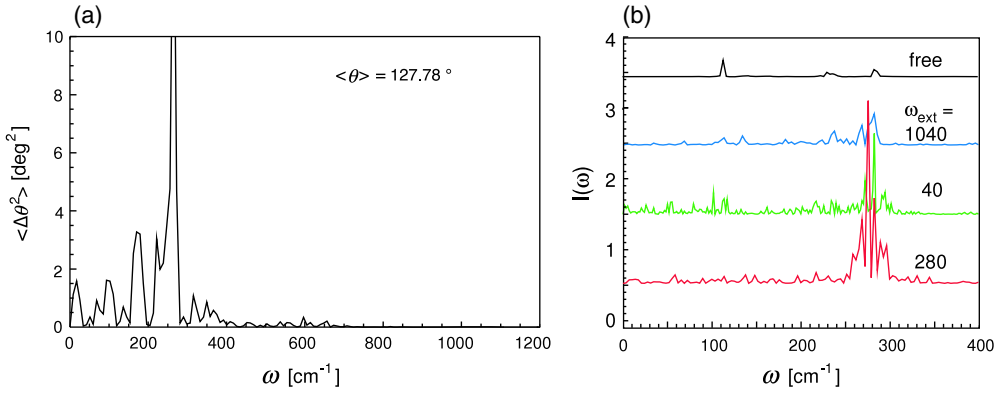

Figure 4. The bending mode of O. (a) Power spectrum of angle deviation $\Delta\theta$ from the equilibrium angle of bond Si–O–Si without IR irradiation. In this case, $\langle T\rangle = 50$ K. (b) Change in the power spectra of $\Delta\theta$ when external forces with a frequency $\omega_{\rm ext}$ are applied. $T_{\rm bath} = 300$ K.

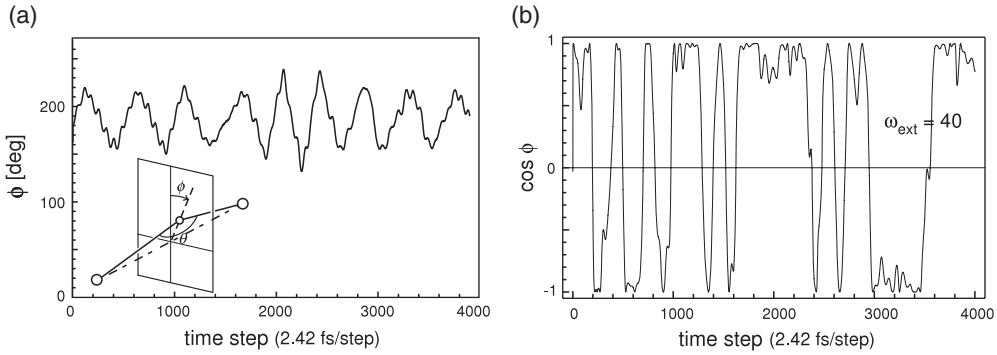

Figure 5. The libration mode of O. (a) Time evolution of the azimuthal angle ϕ is plotted, when no external force is applied. In this case, $\langle T\rangle = 50$ K. (b) Excitation of the librational mode with $\omega_{\rm ext} = 40$ cm^{-1}. $T_{\rm bath} = 300$ K. $\cos\phi$ is plotted.

3.2. Excitation of low-lying modes

Another interesting case is the excitation of low-lying modes. At a point at which low-lying modes are usually buried in the host phonon band, the resonance effect may be inappreciable. However, the amplitude of such low-lying modes is large via the Bose factor, so that it may have some role in diffusion, as in many phase transitions.

Oxygen in Si has low-lying modes. One is the bending mode of the bond angle Si–O–Si. Experimentally, the 517 cm^{-1} band is assigned to this mode [25]. In our simulation, this appears at 280 cm^{-1}, as shown in figure 4. In order to emphasize the bending character, we plot in this figure the spectrum of the deviation of the angle $\Delta\theta$ from the equilibrium angle of the Si–O–Si bond. A large disagreement is present for the frequency $\omega_{\rm B}$ of the bending mode. At present the reason for this disagreement is not clear. The authors do not believe that the small size of the super cell used is sufficient to account for the discrepancy. We can point out that for the Si–O–Si angle, the calculated values in the literature are very largely scattered [26], so that it is no surprise to see such a large discrepancy in $\omega_{\rm B}$. Beside the discrepancy in $\omega_{\rm B}$, the resonance effect is clear, as as shown in figure 4(b). When an external force with $\omega_{\rm ext} = \omega_{\rm B}$, the resonance effect becomes prominent.

Another low-lying mode is a librational mode around the axis Si–O–Si, which is found experimentally at about 30 cm^{-1} [25]. In our simulation, this librational mode appears at about 40 cm^{-1} at low temperatures, as shown in figure 5. At room temperature, this motion becomes circular around the bond axis. Again, in this case, IR excitation with the resonant frequency $\omega_{ext} = 40\ cm^{-1}$ is effective.

4. Summary

FP-MD simulation has been applied to IR excitation of local vibration modes in Si. Although there are severe limitations in terms of timescale and of sampling, we have seen that resonant effects can be reproduced in adiabatic MD simulations by applying an external force on the impurity alone. Nosé thermocontrol is suitable for this study.

This is the first attempt to simulate IR excitation of impurity modes, and it provides a basis for further development. Individual features of impurity modes in the resonant effects will be described on this basis.

Acknowledgments

This work was partly supported by a Grant-in-Aid for Scientific Research in Priority Areas Development of New Quantum Simulators and Quantum Design (no. 17064009) of MEXT, Japan. The computations were performed using the supercomputer facilities of the Cybermedia Center, Osaka University.

References

[1] Fahey P M, Griffin P B and Plummer J D 1989 *Rev. Mod. Phys.* **61** 289
[2] *Proc. 4th Int. Symp. on Advanced Science and Technology of Silicon Materials (Hawaii, November 2004)* (Tokyo: The Japan Society for the Promotion of Science (JSPS))
[3] Yamada-Kaneta H and Tanahashi K 2006 *Physica* B **376/377** 66
[4] Buda F, Chiarotti G L, Car R and Parrinello M 1989 *Phys. Rev. Lett.* **63** 294
[5] Shirai K, Michikita T and Katayama-Yoshida H 2005 *Japan. J. Appl. Phys.* **44** 7760
[6] Budde M, Lüpke G, Parks Cheney C, Tolk N H and Feldman L C 2000 *Phys. Rev. Lett.* **85** 1452
[7] Budde M, Parks Cheney C, Lüpke G, Tolk N H and Feldman L C 2001 *Phys. Rev.* B **63** 195203
[8] Lüpke G, Zhang X, Sun B, Fraser A, Tolk N H and Feldman L C 2002 *Phys. Rev. Lett.* **88** 135501
[9] Sun B, Yang Q, Newman R C, Pajot B, Tolk N H, Feldman L C and Lüpke G 2004 *Phys. Rev. Lett.* **92** 185503
[10] Cowley R A 1964 *Adv. Phys.* **12** 421
[11] Perdew J P and Zunger A 1981 *Phys. Rev.* B **23** 5048
[12] Troullier N and Martins J L 1991 *Phys. Rev.* B **43** 1993
[13] Kleinman L and Bylander D M 1982 *Phys. Rev. Lett.* **48** 1425
[14] http://www.cmp.sanken.osaka-u.ac.jp/∼koun/osaka.html
[15] Angress J F, Goodwin A R and Smith S D 1968 *Proc. R. Soc.* A **308** 111
[16] Shirai K, Hamada I and Katayama-Yoshida H 2006 *Physica* B **376/377** 41
[17] Marques M A L and Gross E K U 2003 *A Primer in Density Functional Theory* ed C Fiolhais, F Nogueira and M Marques (Berlin: Springer) p 144
[18] Bertsch G F, Iwata J-I, Rubio A and Yabana K 2000 *Phys. Rev.* B **62** 7998
[19] Sham L J 1969 *Phys. Rev.* **188** 1431
[20] Resta R 1983 *Phys. Rev.* B **27** 3620
[21] Baroni S and Resta R 1986 *Phys. Rev.* B **33** 7017
[22] Hybertsen M S and Louie S G 1987 *Phys. Rev.* B **35** 5585
[23] Shirai K and Katayama-Yoshida H 2004 *Proc. 4th Int. Symp. on Advanced Science and Technology of Silicon Materials* (Tokyo: The Japan Society for the Promotion of Science (JSPS)) p 129
[24] Nosé S 1984 *J. Chem. Phys.* **81** 511
[25] Yamada-Kaneta H, Kaneta C and Ogawa T 1990 *Phys. Rev.* B **42** 9650
[26] Michikita T, Shirai K and Katayama-Yoshida H 2005 *Japan. J. Appl. Phys.* **44** 7904